A quantitative approach to the loading rate of seismogenic sources in Italy

Alessandro Caporali [1)], Carla Braitenberg [2)], Paola Montone [3)], Giuliana Rossi [4)], Gianluca Valensise [3)], Alfio Viganò [5)], Joaquin Zurutuza [1)]

1) University of Padova, Department of Geosciences

2) University of Trieste, Department of Mathematics and Geosciences

3) Istituto Nazionale di Geofisica e Vulcanologia, Roma

4) Istituto Nazionale di Oceanografia e Geofisica Sperimentale -OGS, Trieste

5) Provincia Autonoma di Trento, Servizio Geologico

GNSS velocities, horizontal strain rates and rate of Coulomb Failure Function

- 550 velocities of GNSS sites resulting from standardized processing compliant with IGS/EUREF Guidelines
- Scattered velocities are converted to strain rates using least squares collocation and at least 4 sites in the neighbourhood of the computation point
- Computation points are chosen as the center of those 85 Individual Seismogenic Sources (ISS) of DISS 3.2.0 of INGV which are sufficently well covered by GNSS data
- Resulting strain rate is projected onto the planes of each selected ISS to comput a normal and tangential strain rate
- Coulomb stress rates on the selected ISS's is computed assuming plane stress rate: it is taken as an indicator of the rate at which regional stress loads known (ISS) faults.

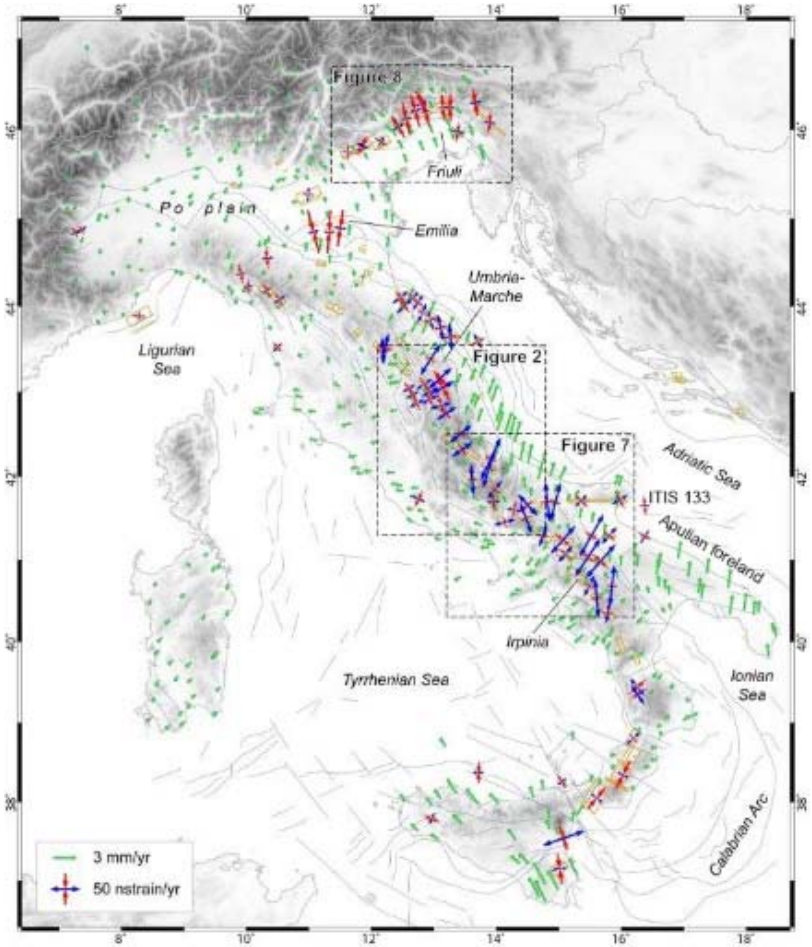

Are ISS faults optimally aligned to the regional stress rate field of GPS?

- Velocities are measured at points; strain rates are estimated for an area covered by velocities
- In the estimate of the strain rate at a point we need to include all the neighboring velocities which define a similar strain rate pattern
- Example for ITIS096 (Isola del Gran Sasso): velocities in a radius of 80 km are maximizing the shear strain rate and define a coherent (mostly) extensional regime. Hence we speak of regional stress/strain rate.
- Normally the eigenvectors of the stress rate from GNSS geodesy agree in direction with both the Sh angles of the Italian stress map (Montone and Mariucci 2016) and the strike of the ISS's
- In this sense we find that the ISS's are optimally oriented to the regional, GNSS inferred strain/stress rate field
- Details in Mastrolembo and Caporali (BGTA 2017)

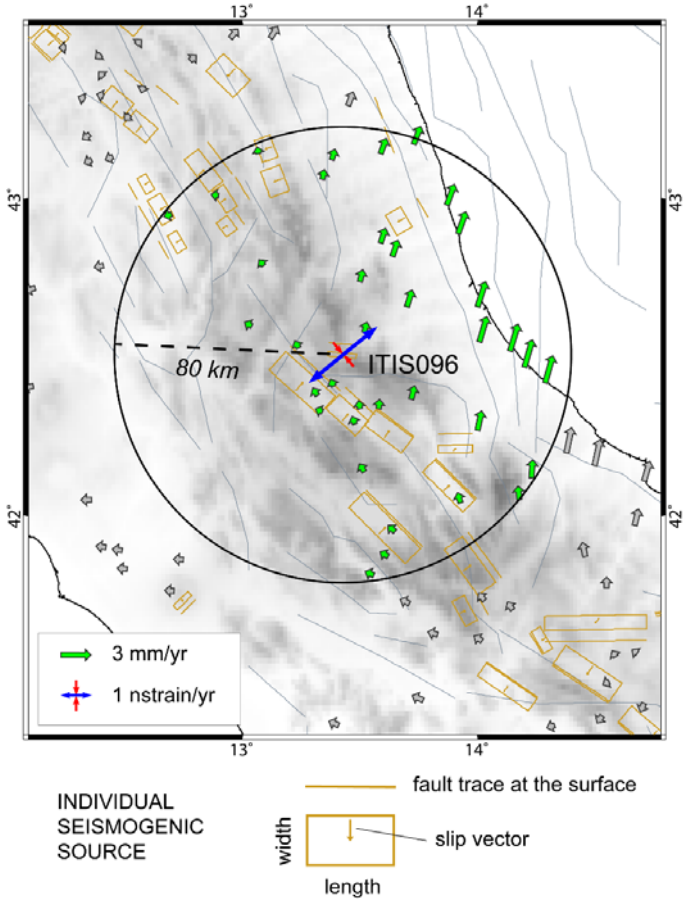

Map of the CFF rate at 85 selected ISS's

- The majority of the studied ISS has a positive rate of CFF (takes stress from the regional field) at a rate between 1 and 3 kPa/yr, assuming a friction of 0.5
- This means that it takes some 300 to 1000 years to obtain a stress of ca 1MPa (10 bar), which is close (in order of magnitude) to a typical stress drop
- This order of magnitude estimate however does not take into account the stress transferred by nearby earthquakes (to be discussed later)
- Central Italy appears to have on average higher CFF rates
- Higher/lower CFF rate does NOT necessarily mean higher/lower seismic hazard

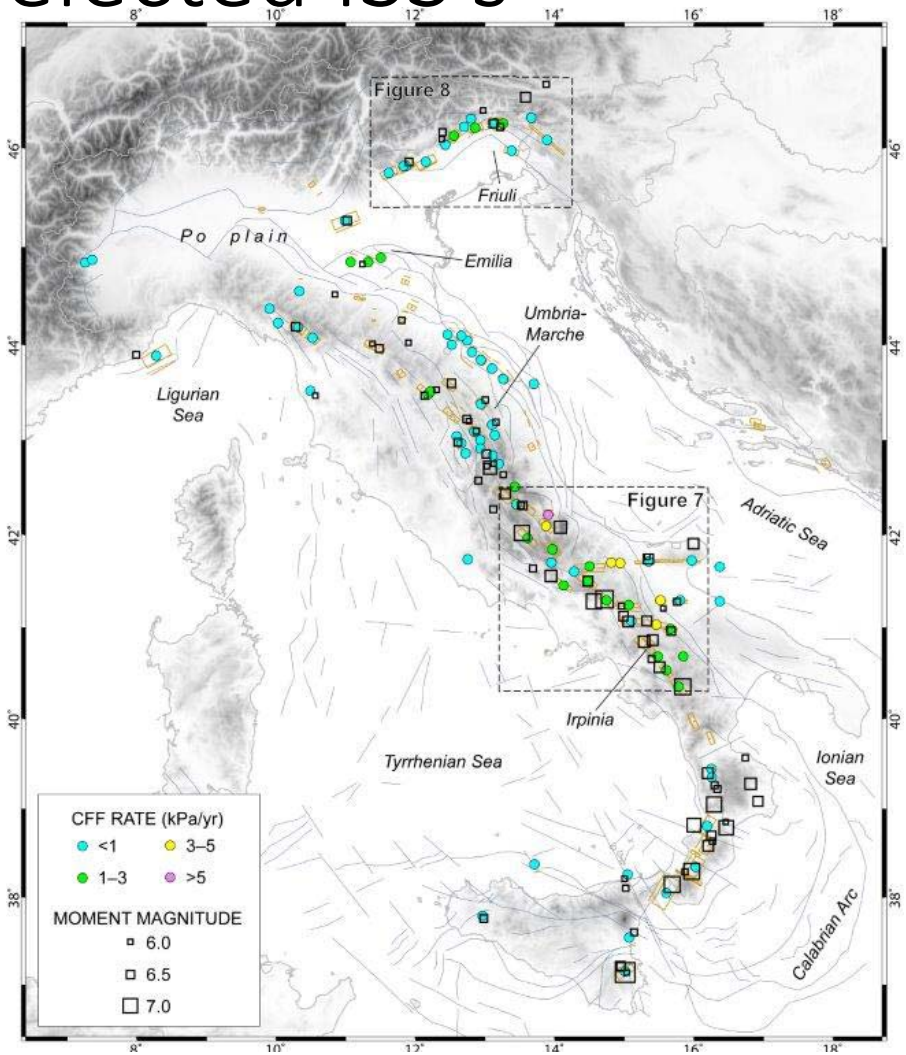

Highest CFF rate found in relatively deep transtensive sources

ITIS094: Tocco da Casauria. This source is associated with the 5-30 December 1456 M=6 earthquakes (Fracassi and Valensise, 2007); ITIS027 (Sulmona) is just south

ITIS052: San Giuliano di Puglia
ITIS053: Ripabottoni
They are both associated with the 2002 Mw 5.7 and 5.8 events at depth of 16-20 km.
SE we find ITIS082 (Ascoli Satriano) and further South ITIS088 (Bisaccia) as yellow

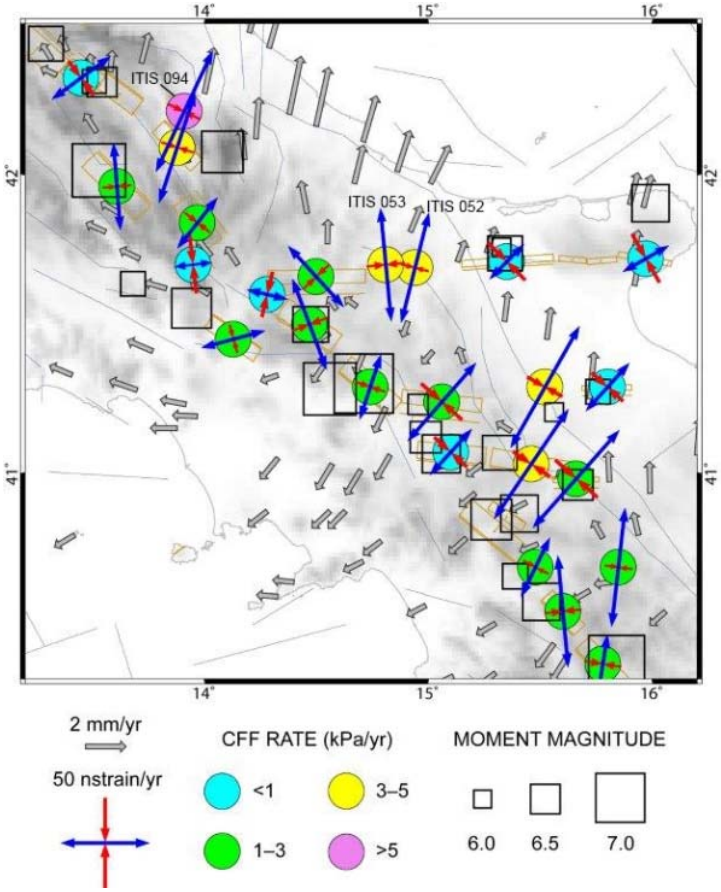

NE Italy

- CFF rate is lower than in Central Italy
- The compressional eigenvector is very well aligned to the strike of the faults especially near the tip of the indenter.

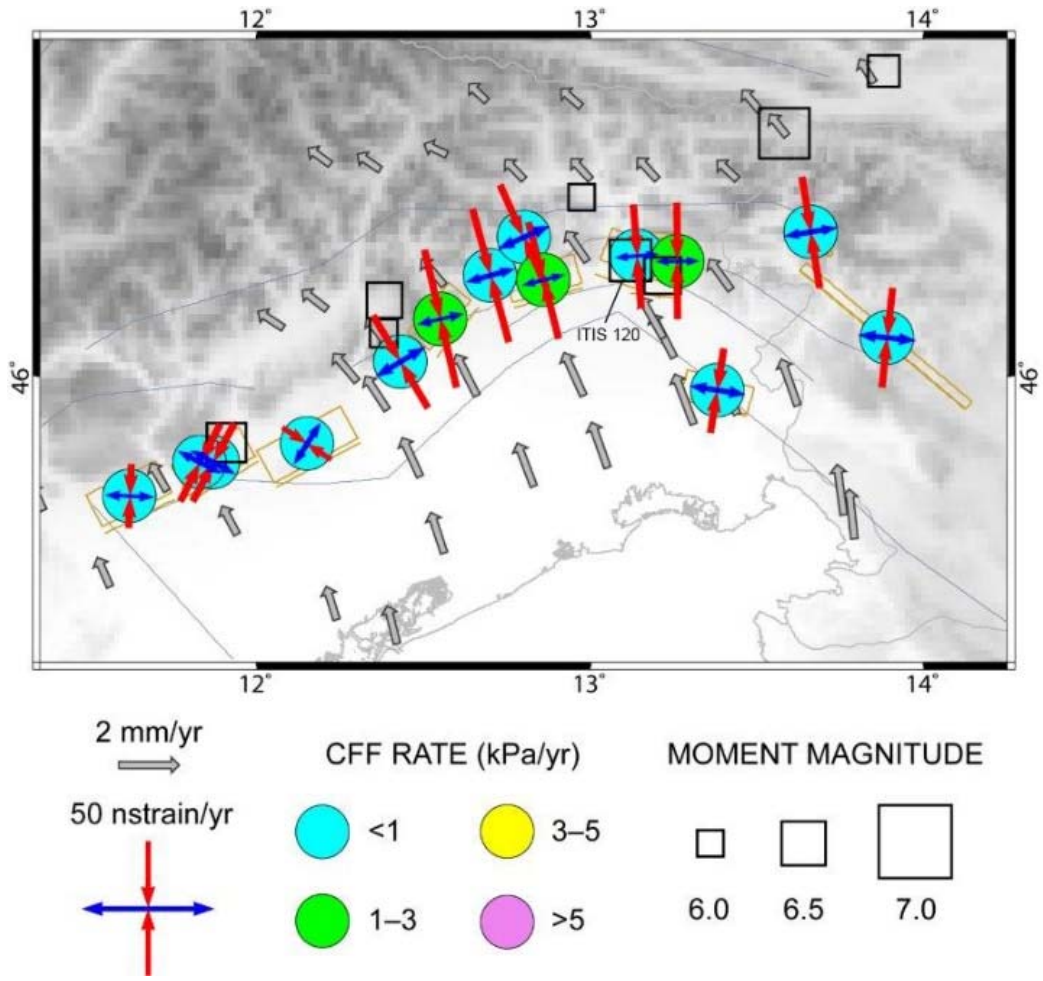

Amatrice and Norcia

Strain rate interpolated at the epicenter of the Amatrice M=6 24.08.2016 event and Norcia M=6.5 31.10.2016 event (both not yet included in DISS 3.2.0)

Rate of CFF at Amatrice/ Norcia is estimated ca. 1 kPa/yr, relatively small

The activated faults appear optimally oriented to the regional stress/strain rate

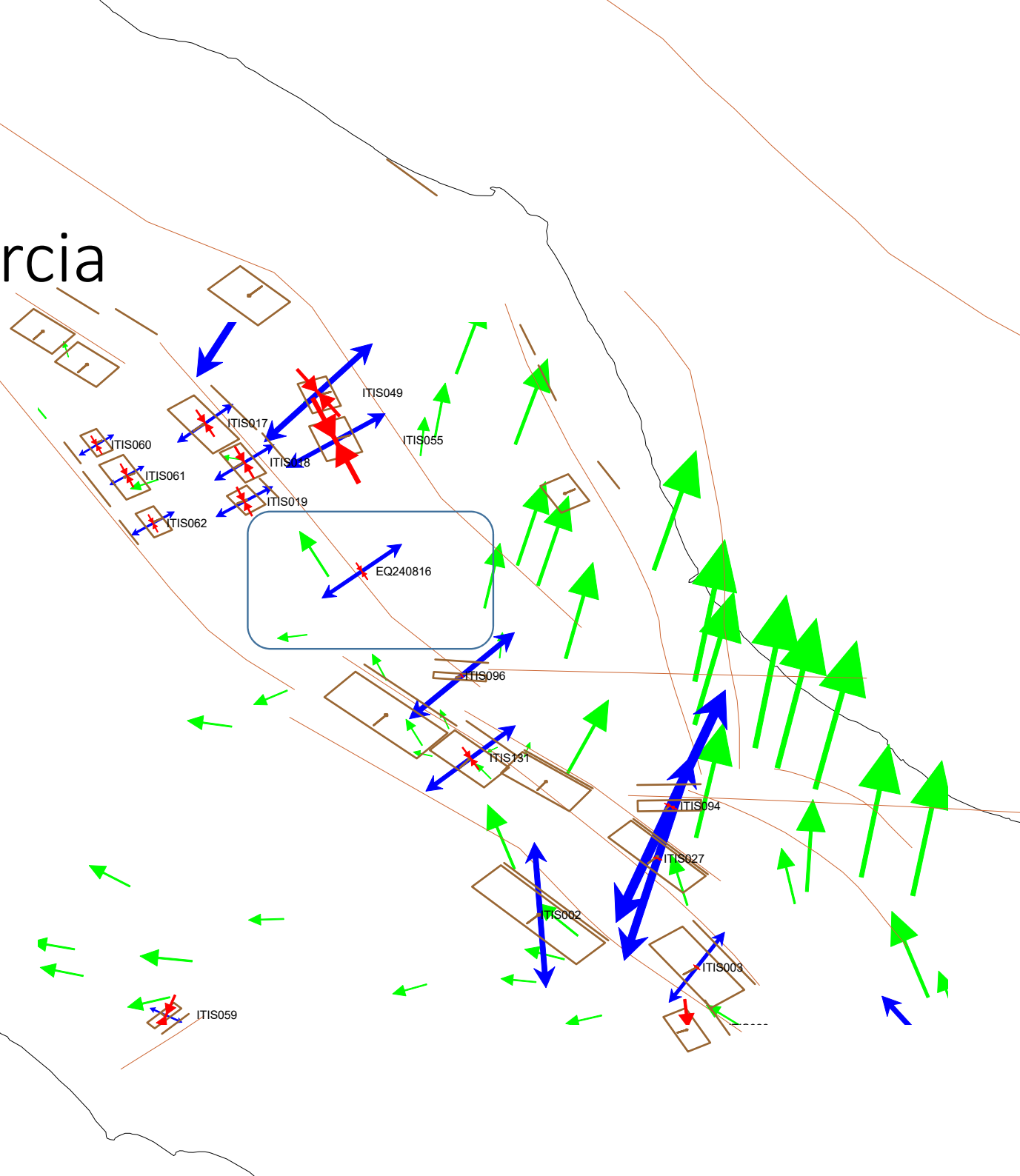

Compilation of events m>6 in Central Italy with known/assumed parameters (DISS+CPTI): how do previous events transfer Coulomb stress to the next event?

Year		X-start	Y-start	X-fin	Y-fin	rt.lat	reverse	dip	top	bot	Source	notes
		km	km	km	km	m	m	deg	km	km		
<1000	1	87.3217	37.2288	100.1459	27.49	0.00	-0.60	50	1	9	ITIS132	San Pio delle Camere
<1000	2	107.7159	19.7079	121.6957	5.58	0.00	-0.66	60	1	12	ITIS027	Sulmona
<1000	3	117.3608	-7.3844	128.9352	-23.55	0.00	-0.66	50	3	12	ITIS003	Aremogna – Cinque miglia
1315	4	113.7159	-1.7079	127.6957	-5.58	0.00	-0.45	60	1	12	CPTI04	SE of Sulmona
1328	5	40.5521	99.3254	44.0842	94.48	0.00	-0.65	40	3	7	CPTI04	NW of Norcia
1349	6	81.6242	26.7731	91.7816	17.24	-0.05	-0.60	43	3	10	CPTI04	S of Paganica
1456	7	108.9243	24.7949	120.8066	25.00	0.29	-0.34	70	11	19	ITIS094	Tocco da Casauria
1461	8	74.6242	42.7731	84.7816	33.24	-0.05	-0.65	43	3	10	CPTI04	Aquila replica?
1639	9	63.35	75.29	71.81	57.16	-0.01	-0.60	49	4	12	CPTI04	S of Amatrice
1703	10	47.02	89.99	59.85	66.84	-0.01	-0.69	47	1	9	CPTI04	N of Montereale January
1703	11	55.9697	57.7176	73.2484	42.08	0.00	-0.72	50	3	13	ITIS015	Montereale February
1741	12	34.3678	161.3795	43.6455	152.20	0.00	0.55	20	14	17	ITIS048	Fabriano
1799	13	50.4563	133.1716	53.2076	125.66	0.00	0.40	20	14	16	ITIS049	Camerino
1832	14	12.9727	101.7026	7.8604	110.53	0.00	-0.35	30	2	5	ITIS061	Foligno
1854	15	7.4237	112.6747	4.3123	118.04	0.00	-0.20	30	2	4	ITIS060	Bastia
1873	16	53.9451	122.8294	57.2068	113.91	0.00	0.50	20	14	17	ITIS055	Sarnano
1878	17	18.182	92.0267	14.6794	98.08	0.00	-0.25	30	2	4	ITIS062	Trevi
1915	18	83.2717	8.2693	102.8022	-11.51	0.00	-1.06	60	2	15	ITIS002	Fucino
1943	19	95.9116	108.1986	99.8687	101.36	0.00	0.40	35	5	9	ITIS070	Offida
1950	20	70.6712	57.6663	80.5836	56.80	0.18	-0.18	75	12	18	ITIS096	Isola del Gran Sasso
1984	21	3.8434	141.9438	11.5549	135.52	0.00	-0.50	20	4	6	ITIS037	Gubbio_South
1997	22	34.4005	116.1134	39.1838	108.4893	-0.05	-0.38	40	4	8	ITIS018	Colfiorito_1
1997	23	25.6479	128.3408	34.1103	117.1722	-0.03	-0.33	40	3	9	ITIS017	Colfiorito_2
1997	24	35.5521	105.3254	39.0842	100.4766	0.05	-0.28	40	3	7	ITIS019	Colfiorito_3
2009	25	74.6242	42.7731	84.7816	33.2356	-0.05	-0.60	43	3	10	ITIS131	Paganica
2016	26	58.35	88.29	66.81	70.16	---0.01	-0.19	49	4	12	EQ24082016	Amatrice
2016	27	47.02	106.99	59.85	83.84	-0.01	-0.65	47	1	9	EQ30102016	Norcia

Coulomb stress pre and post the 2009 event at 3 km depth

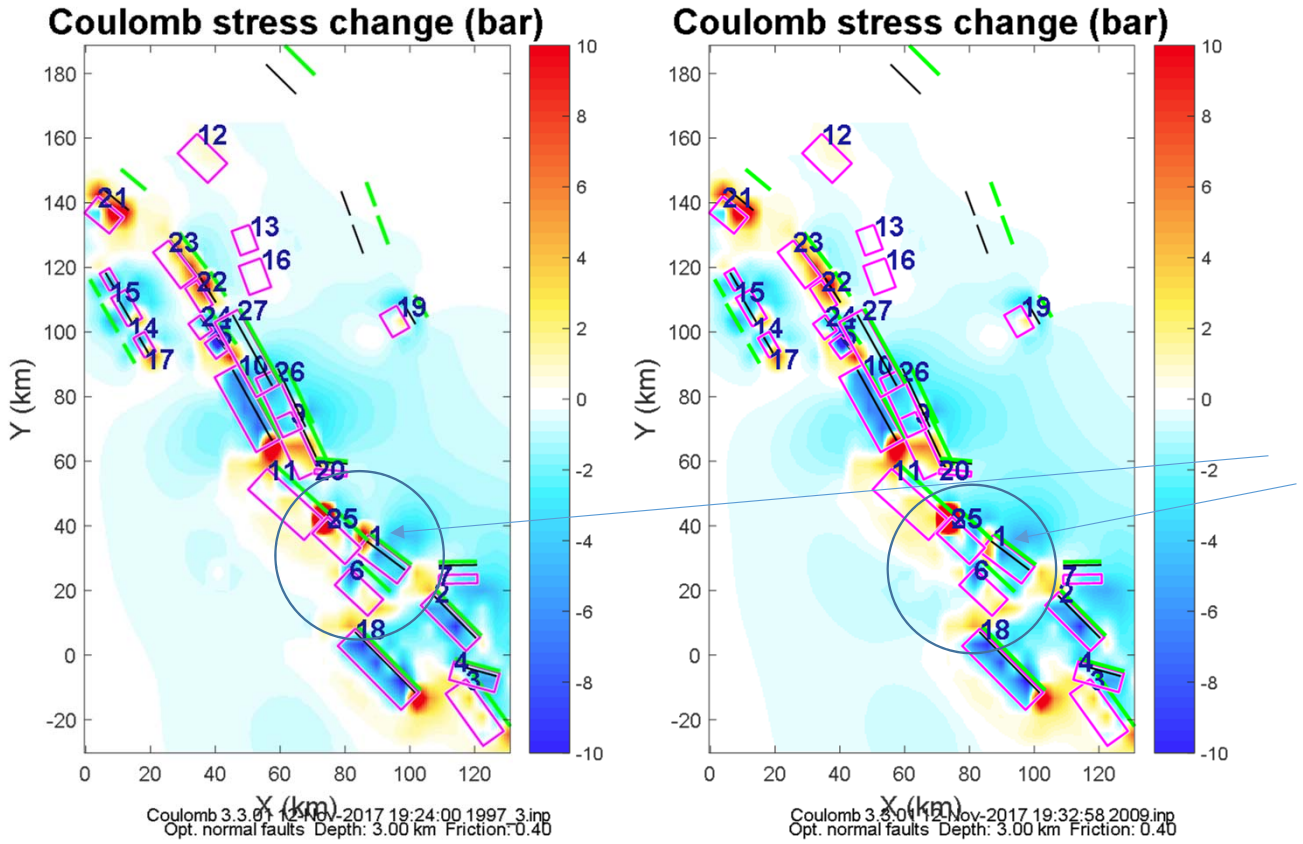

The map shows the state of Coulomb stress in Central Italy before and after the Aquila event of 2009 (Paganica fault is n.25)

The positive Coulomb stress which is released is at the border between the Paganica (25) and San Pio delle Camere (1) faults
High Coulomb stress at the border between Paganica (n.25) and Montereale (n.11)

Coulomb stress pre and post the 2009 event at 3.5 km depth

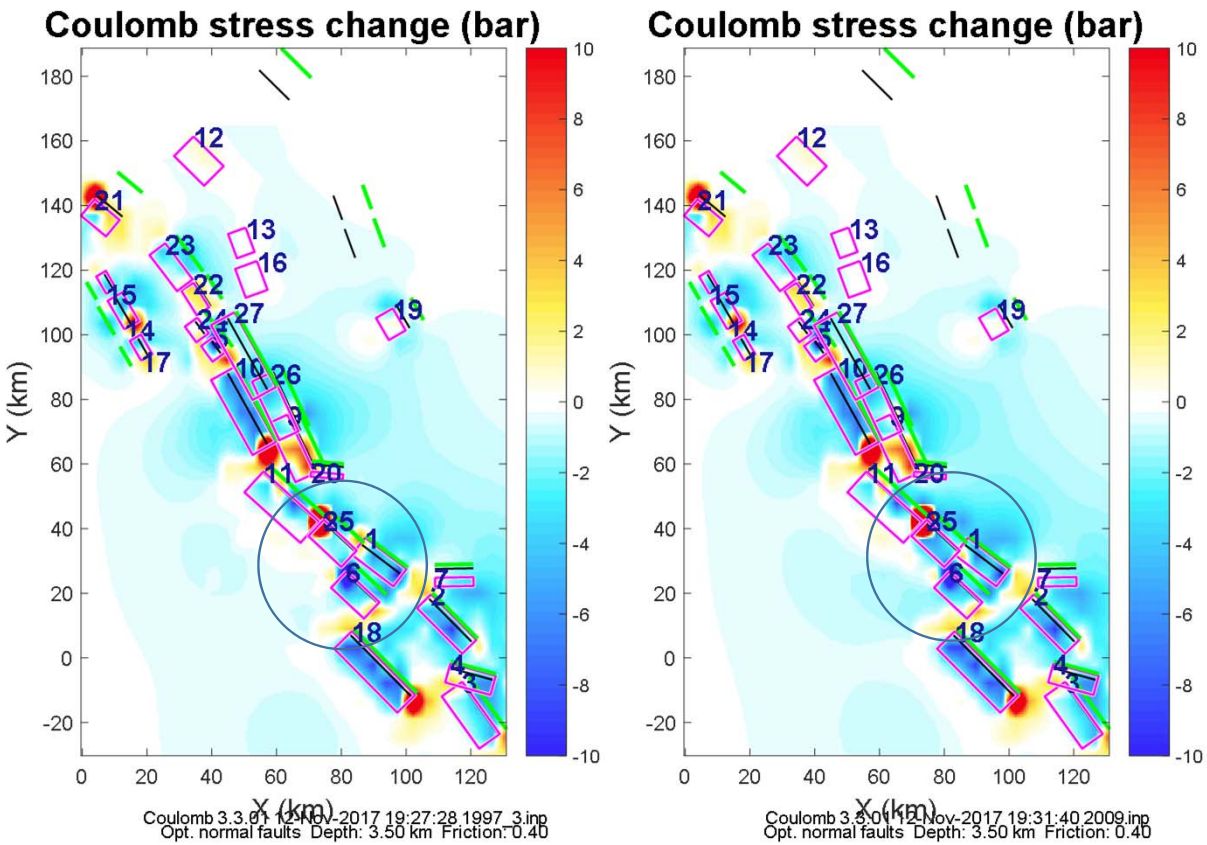

The map shows the state of Coulomb stress in Central Italy before and after the Aquila event of 2009 (Paganica fault is n.25)

Coulomb stress pre and post the 2009 event at 4 km depth

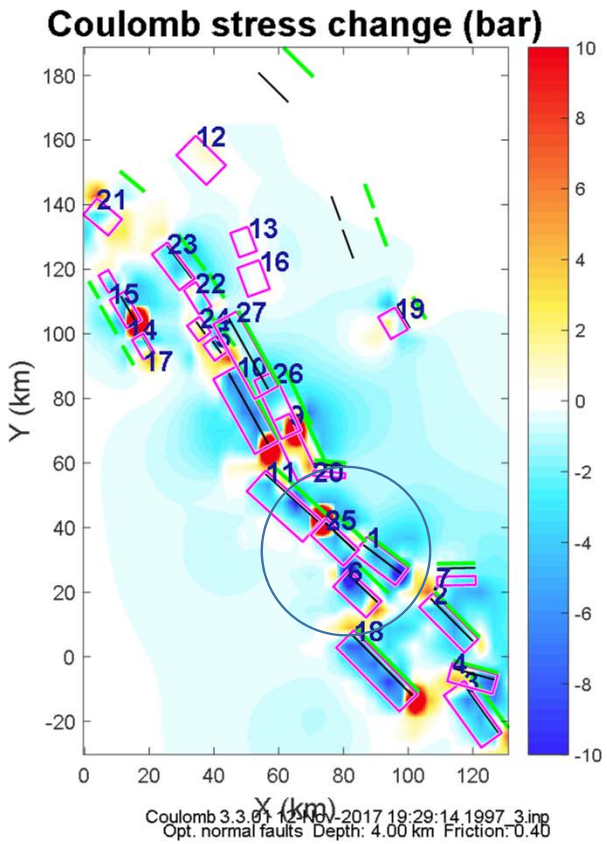

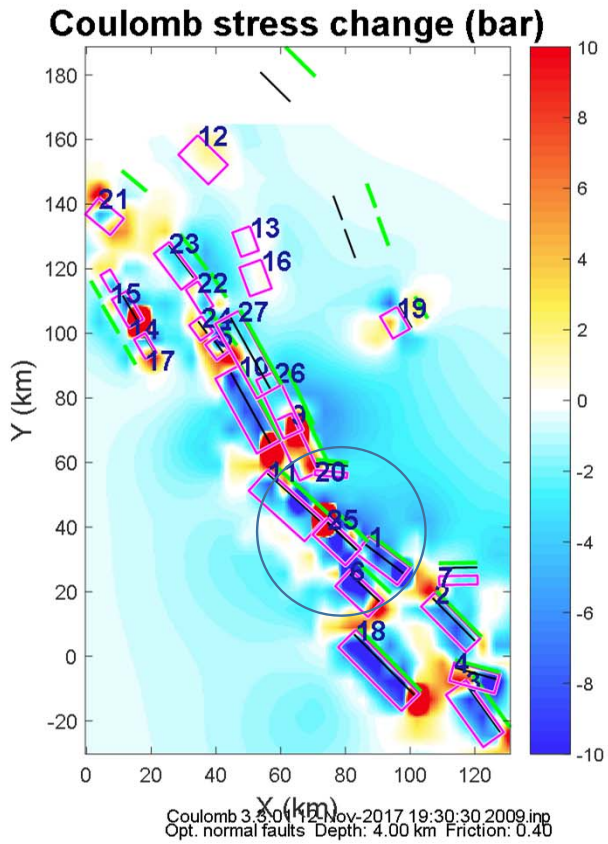

The map shows the state of Coulomb stress in Central Italy before and after the Aquila event of 2009 (Paganica fault is n.25)

At 4km depth there is the largest decrease of Coulomb stress

Major active faults are described in the DISS database of INGV

Stress is accomodated by SW dipping normal faults, which are optimally oriented to the regional stress rate field ca. N50E (measurable with GNSS)

The regional field is complemented by a Coulomb field originating from past earthquakes and mapped to optimally oriented faults

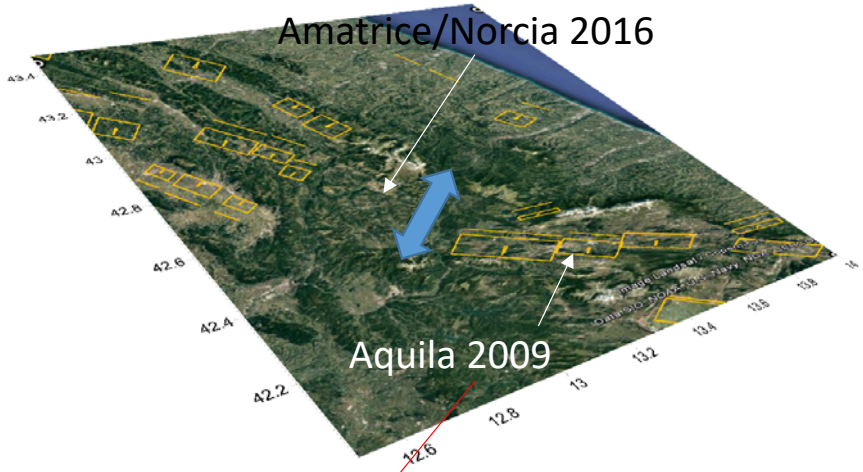

Red rectangles are sources from the DISS of INGV. View from SE to NW

The map to the right shows the very patchy Coulomb stress distribution in the depth range 0:25 km computed using the Okada model and fault plane solutions of events of m>6 occurred from 1315 to 2016, according to CPTI15 and DISS

Volumes where the Coulomb stress is highest should correlate with microseismicity

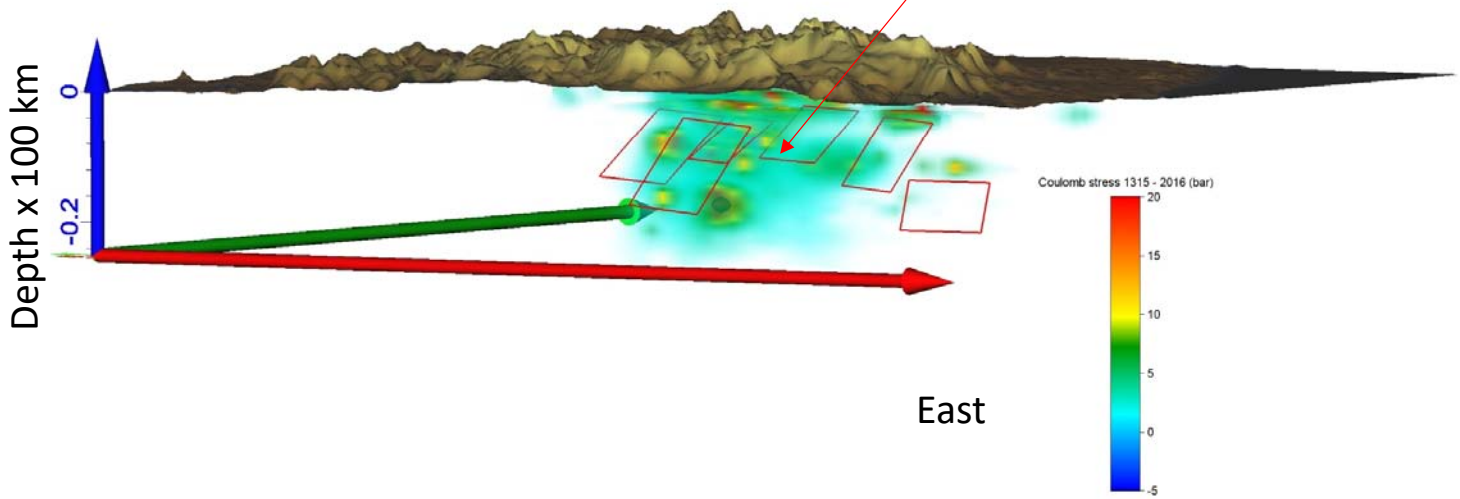

Conclusions

- Coulomb loading rate on ISS's has been mapped with an accuracy better than 1 kPa/yr
- Highest loading rates found on ITIS094 Tocco da Casauria, ca 5 kPa/yr
- Lower rates in Friuli
- High/low loading rate does not necessarily mean high/low seismic hazard
- Stress transfer of individual earthquakes and regional stress generate comparable loads on faults
- It is conceivable to map crustal stress summing the two contributions

Coseismic displacement (daily solutions): vertical (left), horizontal (right)

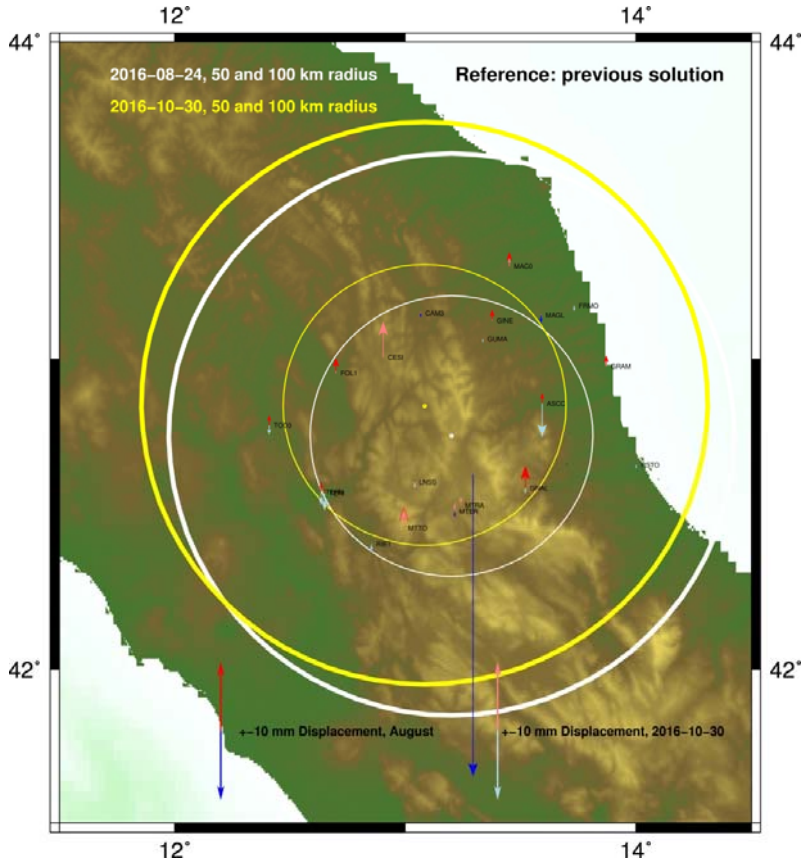

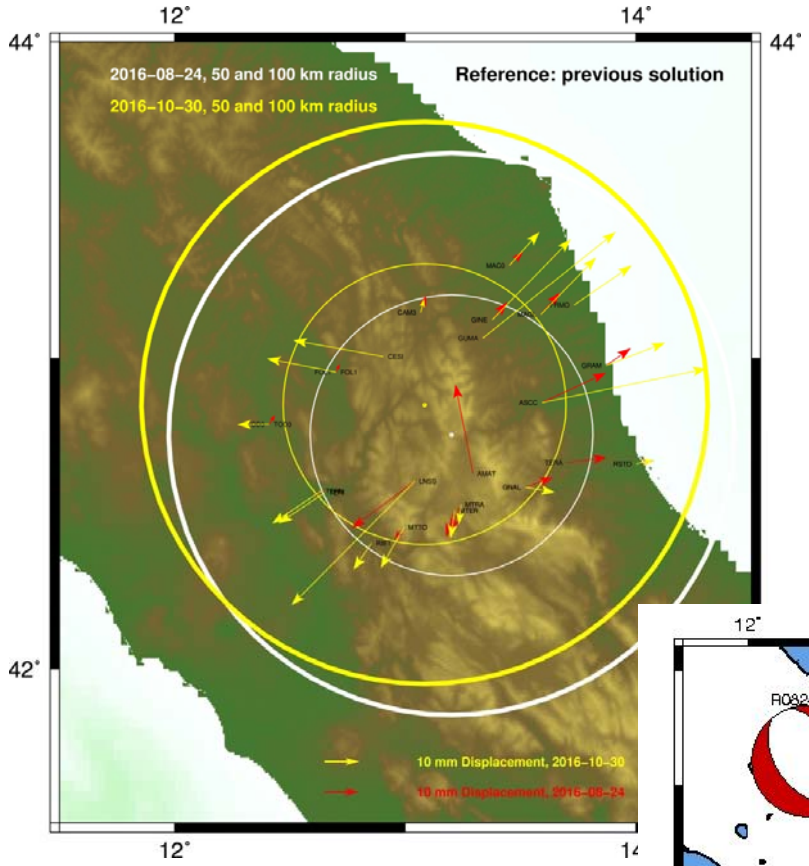

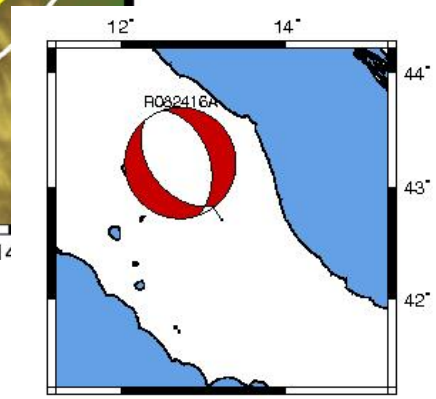

Visit our web site http://147.162.183.196/Earthquake/EQ_monitor.htm daily updated

Example of time series (daily staking of normal equations of the full network (+600 sites) aligned to EUREF Class A sites

- Signal : continuous line
- Noise: residuals after removal of continuous line

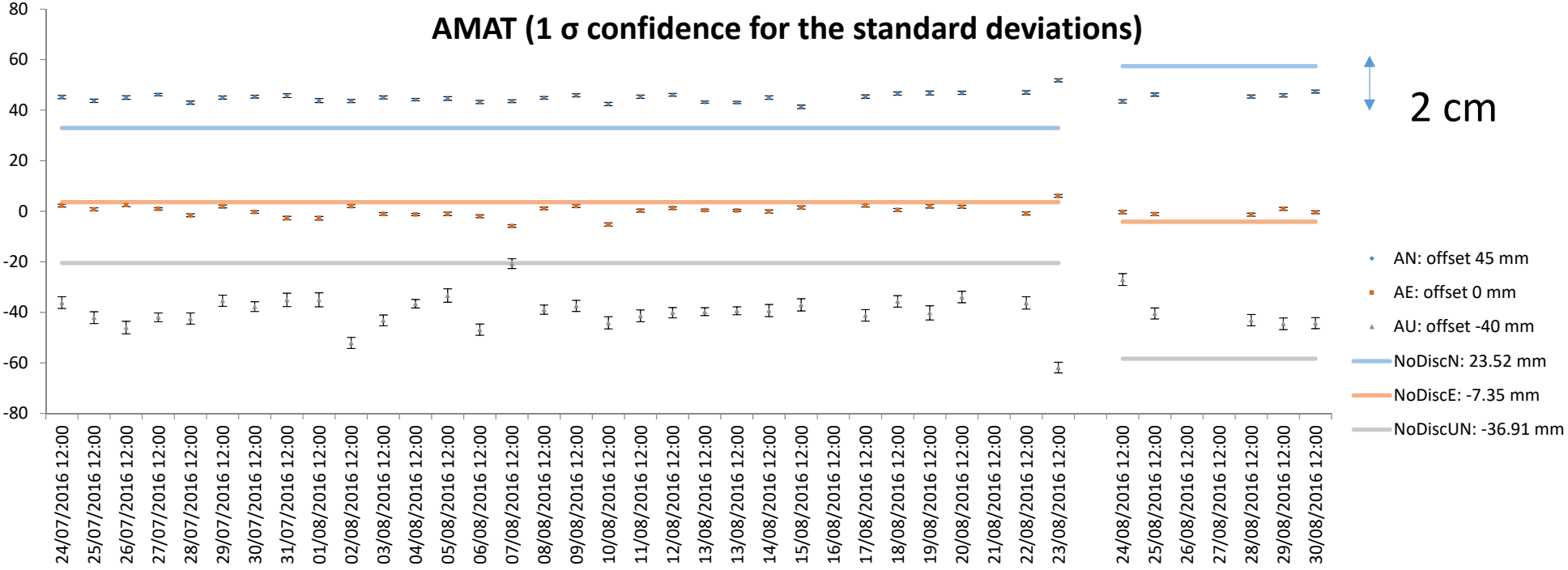

Analysis in a semi infinite elastic half space (Okada)

- Blue arrows= measured
- Red arrows= modeled using INGV/Time Domain Moment Tensor (TDMT)

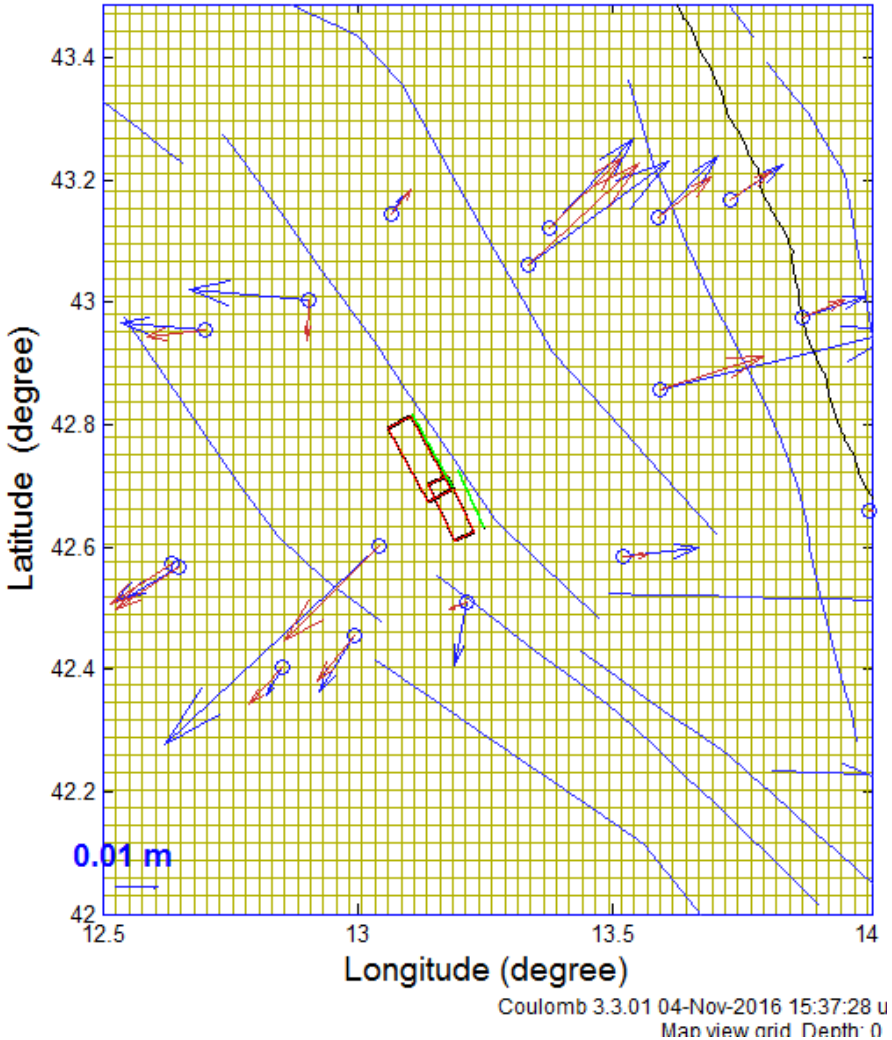

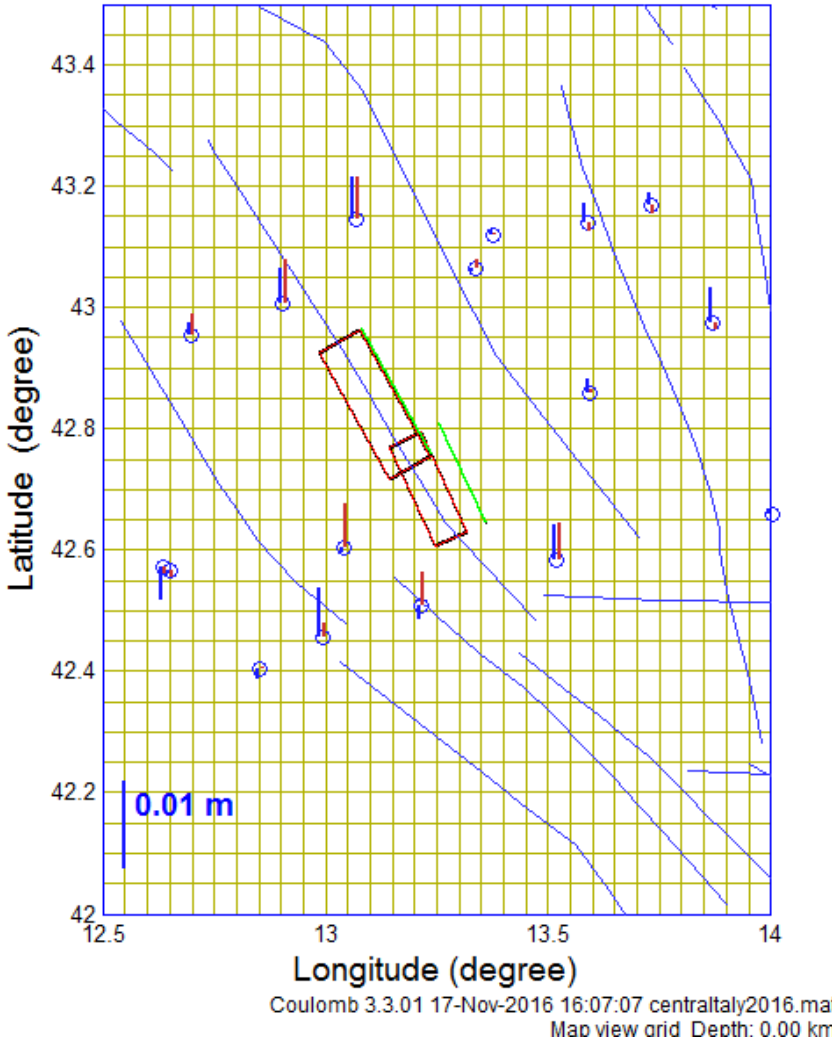

Using GNSS data to discriminate among several seismological solutions

- Observed displacements by GNSS are very sensitive to epicentral coordinates and fault orientation
- Several seismic analysis centers publish epicentral coordinates and fault parameters based on the arrival times of P and S waves at a network of seismic stations (infrastructure similar to EPN!)
- These seismic solutions can be used to generate predictions of surface displacements in 3D of the nearest GNSS sites, to be compared with the measured displacements (within ca. 40 km, for m_w=6.2 : 6.5)
- We have tested GFZ, QuickCMT (Harvard) and INGV, and concluded that the latter is slightly better than the others
- This analysis is an example of synergy between infrastructures using different technologies to monitor seismic events

Hor/Ver displacement of GNSS stations as a function of their distance from epicenter: GNSS observed vs. seismic model

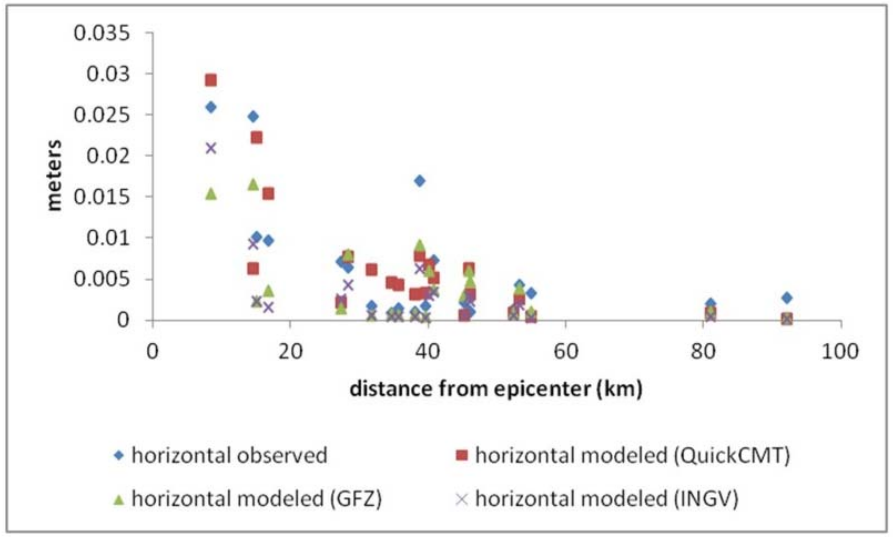

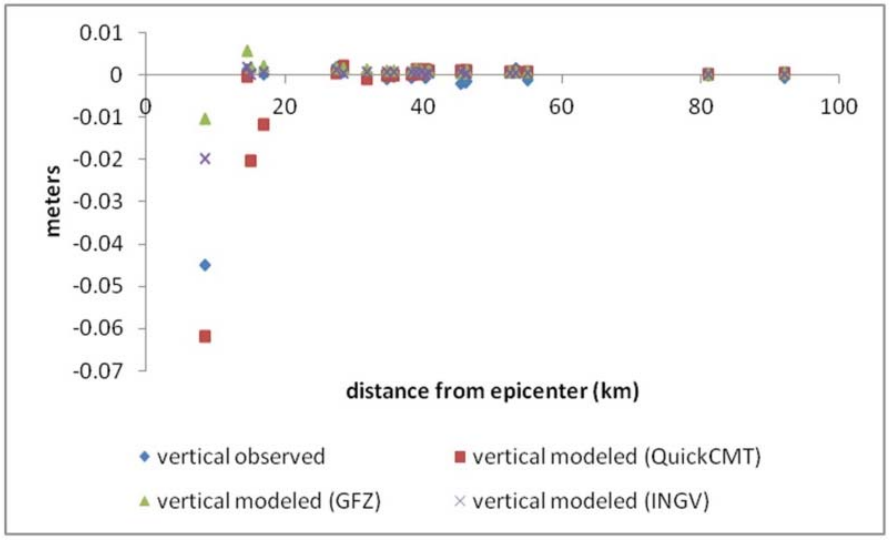

Expected vertical displacement, for comparison with InSAR data

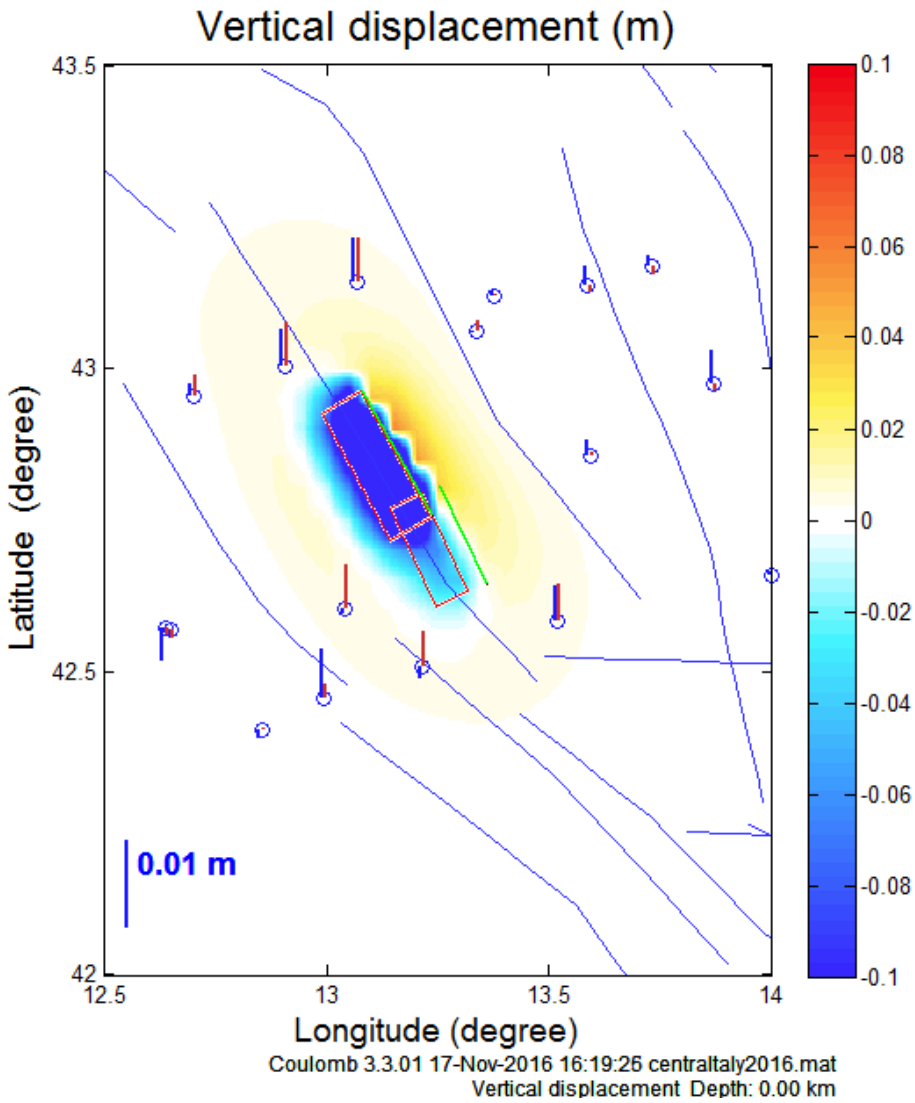

Conclusions

- Analysis of the long term stress field based on GNSS data indicates that the epicentral area is subject to a non zero extensional stress rate, but lower than e.g. in Tocco da Casauria: regional stress may not be a unique indicator of hazard
- Optimal alignment of the GNSS inferred extensional eigenvector to major structures
- GNSS provides an extremely quick response in terms of accurate coseismic displacements
- Surface data are most sensitive to hypocenter location than to angles, tessellated in plane displacements
- Ready for inclusion of InSAR data